Resistance to RevM10 inhibition reflects a conformational switch in the HIV-1 Rev response element

Michal Legiewicz*†, Christopher S. Badorrek*†, Kevin B. Turner‡, Daniele Fabris‡, Tiffany E. Hamm§, David Rekosh§, Marie-Louise Hammarskjöld§, and Stuart F. J. Le Grice*¶

*HIV Drug Resistance Program, National Cancer Institute, Frederick, MD 21702; ‡Department of Chemistry and Biochemistry, University of Maryland Baltimore County, Baltimore, MD 21250; and §Myles Thayler Center for AIDS and Human Retrovirus Research and Department of Microbiology, University of Virginia, Charlottesville, VA 22908

Edited by Stephen P. Goff, Columbia University College of Physicians and Surgeons, New York, NY, and approved July 28, 2008 (received for review May 8, 2008)

Nuclear export of certain HIV-1 mRNAs requires an interaction between the viral Rev protein and the Rev response element (RRE), a structured element located in the Env region of its RNA genome. This interaction is an attractive target for both drug design and gene therapy, exemplified by RevM10, a transdominant negative protein that, when introduced into host cells, disrupts viral mRNA export. However, two silent G->A mutations in the RRE (RRE61) confer RevM10 resistance, which prompted us to examine RRE structure using a novel chemical probing strategy. Variations in region III/IV/V of mutant RNAs suggest a stepwise rearrangement to RevM10 resistance. Mass spectrometry was used to directly assess Rev ''loading'' onto RRE and its variants, indicating that this is unaffected by RNA structural changes. Similarity in chemical footprints with mutant protein implicates additional host factors in RevM10 resistance.

chemical footprinting | HIV RNA evolution | mass spectrometry | Rev/RRE interaction

Export of a subset of HIV-1 mRNAs is a crucial process in the life cycle mediated by the Rev protein. Although completely spliced viral mRNA is transported to the cytoplasm without a need for Rev, export of unspliced or partially spliced transcripts mandates binding of Rev to the Rev response element (RRE), a structural feature present in these RNA species. The Rev-RRE complex subsequently interacts with cellular factors, such as CRM1 (1, 2); Ran-GTP (3); and, perhaps, eIF-5A (4), to facilitate export.

The Rev nuclear localization signal (NLS), located near the N terminus, is an arginine-rich domain (5) that mediates import (6) and RRE binding (7, 8). The NLS is also flanked by regions implicated in Rev multimerization (9, 10). The nuclear export signal (NES), located near the C terminus, is a leucine-rich domain (11, 12) that interacts with the nuclear export factor CRM1 (2). Because Rev function is vital for viral replication, it is an attractive target for drug design and gene therapy. In one study, a Rev variant (RevM10), carrying two mutations in the NES, induced a transdominant negative phenotype and, when introduced into human T-cells, disrupted export of Rev-dependent viral mRNAs (13). A number of gene therapy vectors (14–16) have been devised to deliver RevM10, and a phase 1 clinical trial was been performed in ref. 14.

The precise mechanism by which RevM10 inhibits Rev function is unknown. Selection for viral resistance in infected cell cultures, using virus derived from the NL4–3 molecular clone, demonstrated, surprisingly, that silent mutations at nucleotides (nts) 164 (G:A164) and 245 (G:A254) in the RRE (designated RRE61) induced resistance to RevM10 (17). Because the Env sequence is unaffected by these mutations, this implies structural differences in the mutant RNA. We therefore used selective 2′-hydroxyl acylation analyzed by primer extension (SHAPE) (18) to derive secondary structures of WT and mutant RREs at single nucleotide resolution.

Our work illustrates that the two silent G:A mutations create an RRE with structural alterations in region III/IV/V. The G:A164 mutation enforces a two stem-loop motif in region III/IV but *in vitro* fails to confer RevM10 resistance, whereas the G:A245 mutation alone was sufficient to invoke the RRE61 structure. Through our analysis of mutations constituting the RRE61 phenotype, we propose that the NL4–3 isolate of HIV-1 achieves resistance to RevM10 by stepwise altering RRE structure. We also used mass spectrometry and SHAPE to monitor the stoichiometry and position of Rev binding to the native and RRE61 RNAs, respectively. The former approach indicates that Rev binding to RRE61 is unaltered by the structural change and that Rev binds the WT and mutant RREs in monomeric increments. A complementary SHAPE analysis also indicates that Rev and *trans*-dominant RevM10 binding affects the same nucleotides in the primary Rev binding site of both the WT and RRE61 RNAs. Our observation that silent nucleotide changes can dramatically affect structure and function illustrates the dynamic nature of the RRE.

Results

Structure of WT RRE and RevM10-Resistant RNAs. Native and RRE61 RNAs derived from pNL4–3, containing a 3′ non-viral structure cassette (18), were prepared by *in vitro* transcription. The RRE used here is defined by pNL4–3 nucleotides 7760–7992 (GenBank accession no. AF324493). For comparative purposes, it is described here as nucleotides 60–292 based on the RRE sequence of Charpentier *et al.* (19), and fully functional in reporter assays. RNAs were folded alone or with varying concentrations of Rev and analyzed by non-denaturing gel electrophoresis [supporting information (SI) Fig. S1]. Although the affinity of Rev for the two RNAs was not significantly different, RRE61 RNA and its Rev-containing complexes migrated slower (Fig. S1), suggesting that it adopted an alternative conformation.

Because RRE and RRE61 migrated as homogeneous species, their structures were determined by SHAPE (18), which assesses local flexibility in RNA via accessibility of the 2′-OH group to N-methylisatoic anhydride (NMIA). In flexible regions (i.e.,

Author contributions: D.R. and M.-L.H. designed research; M.L., C.S.B., K.B.T., D.F., and T.E.H. performed research; M.L., C.S.B., K.B.T., and D.F. analyzed data; and M.L., C.S.B., D.R., M.-L.H., and S.F.J.L.G. wrote the paper.

The authors declare no conflict of interest.

This article is a PNAS Direct Submission.

†M.L. and C.S.B contributed equally to this work.

¶To whom correspondence should be addressed. E-mail: slegrice@ncifcrf.gov.

This article contains supporting information online at www.pnas.org/cgi/content/full/0804461105/DCSupplemental.

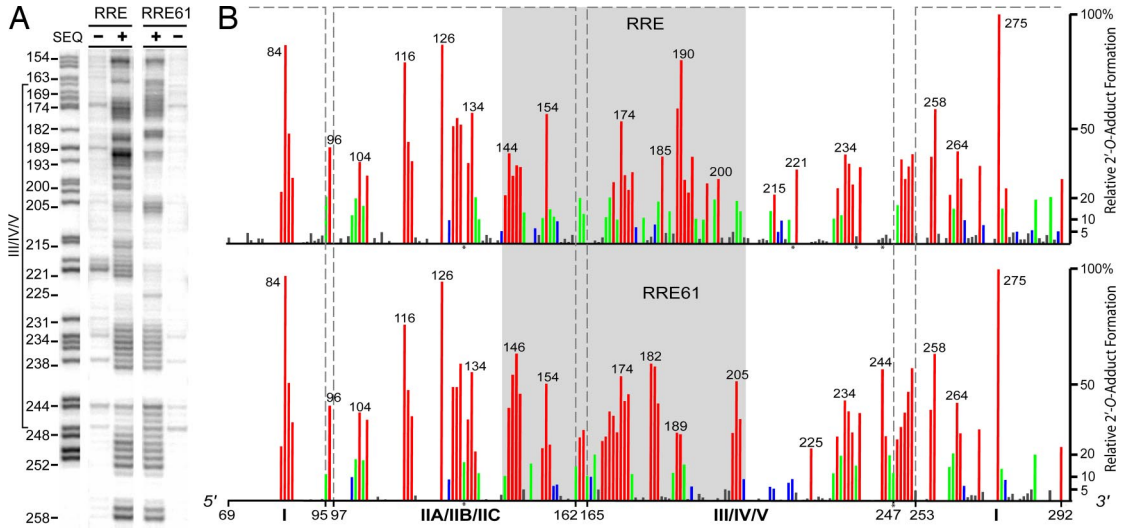

Fig. 1. NMIA footprinting of the WT HIV-1 RRE and RRE61. (*A*) 2′-*O* adduct formation for region III/IV/V of each RNA. (*B*) Histograms depicting absolute SHAPE reactivities. The shaded region indicates where the RNAs differ in NMIA reactivity. Positions of high (>21%) reactivity are in red, those of moderate (10–21%) reactivity are in green, those of low (5–10%) reactivity are in blue, and those of nonreactive (<5%) reactivity are in black. Asterisks indicates where NMIA reactivity was affected by background.

loops, bulges, junctions, etc.), the RNA adopts conformations allowing formation of a nucleophilic 2′-oxyanion that reacts with NMIA to form a bulky 2′-*O* adduct (Fig. S2). Primer extension with an end-labeled DNA primer creates a cDNA library corresponding to stops at sites of adduct formation in the RNA when analyzed by high resolution gel electrophoresis.

Fig. 1*A* shows the sites of adduct formation for both RNAs. Band intensities were quantified at every site and absolute reactivity computed by subtracting the background of the sample lacking NMIA. Using the reactivity profile of an RNA cassette of known structure, we normalized both RNAs to generate histograms highlighting reactivity at each position (Fig. 1*B*).

Structure of the Native RRE. We classify NMIA reactivity as high (>21%), moderate (10–21%), low (5–10%), and nonreactive (<5%), which is used to constrain the folding prediction algorithm RNAstructure 4.4. A position with reactivity >21% is defined as single-stranded, whereas 10–21% would be either single-stranded, adjacent to a G-U pair in the stem or adjacent to a single-stranded nucleotide (e.g., a bulge, junction, top of stem). The predicted model was then obtained based upon SHAPE data (Fig. 2). Reactivities were superimposed on our predicted secondary structure model of the native RRE (Fig. S3).

Analysis of the native RRE confirms four structured regions: I, IIA/IIB/IIC, and III/IV and V (19, 20). Region I comprises a single large anchoring stem spanning nts 60–95 and 253–291. High to moderate NMIA reactivity is observed at nucleotides 83–86, 258, 263–265, 270, 275, and 285, corresponding to bulges in the stem. However, high and moderately reactive nucleotides were also noted at nucleotides 95, 257, 262, 276, and 277. In SHAPE, this is occasionally observed at the end of helices, in particular the 3′ end, but if the partner opposite the reactive nucleotide is non- or moderately reactive, then the pair is represented as existing in a secondary structure. In our case, high reactivity is noted at nucleotides 257 and 262, but no reactivity is seen at their pairing partners C91 or G87; thus, the pairs are represented as shown. Moderate hits at nucleotides 95 and 276 are adjacent to highly reactive A96 and A275 bulges and thus are accepted by the parameters set by the structure prediction algorithm. A275 is one of the most reactive positions in the RRE. This single bulged base is flanked on one side by two A-U pairs and on the other by a G-U pair, which appears to increase the local flexibility of A275 and its accessibility to NMIA.

Region IIA/IIB/IIC spans nucleotides 97–162 containing the stem duplex IIA and stem loops IIB and IIC. Again, high to moderate NMIA reactivity at nucleotides 102–106, 116–118, 126, 129–136, 143–148, and 153–156 indicates both stem-loops

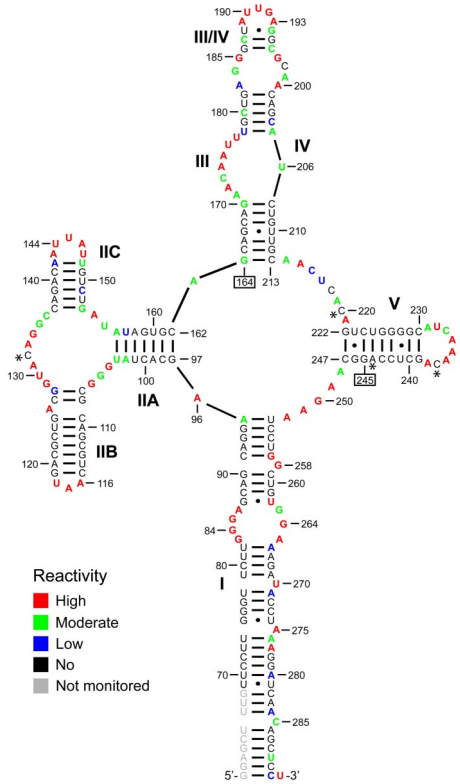

Fig. 2. Secondary structure model for the RRE RNA. The structure is shown with color-coded nucleotides defining NMIA reactivity as indicated in the insert and is consistent with Fig. 1 coding. The G:A164 and G:A245 mutations are boxed.

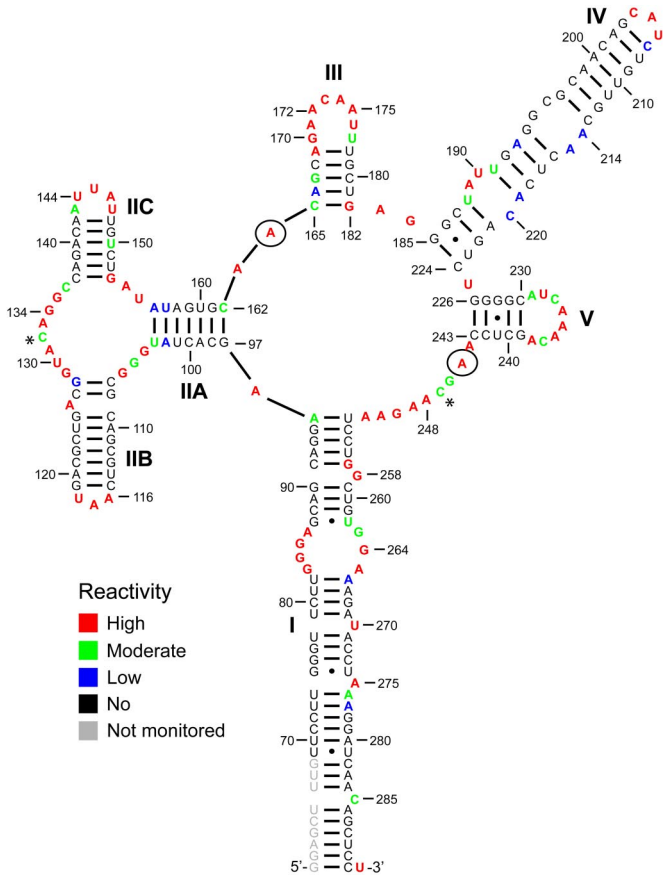

Fig. 3. Secondary structure model for the RRE61 RNA. Color coding of nucleotide reactivity follows the legend to Fig. 2. The two G:A mutations are now incorporated into the structure and are highlighted with open circles.

and bulges. Region III/IV/V spans nucleotides 164–252 and contains two stem-loops (III/IV and V). As expected, almost all high and moderate NMIA-reactive nucleotides of this domain are within stem-loops, bulges, and junctions of the RNA. We also observed minimal reactivity at nucleotides 216–218, located between stem III/IV and stem V, raising the possibility this site might participate in long-range interactions.

Structural Changes in Region III/IV/V of RRE61. As indicated earlier, RRE61 RNA migrated slower than WT RRE during nondenaturing gel electrophoresis. (Fig. S1). Consistent with this observation, RRE61 acquired a different 2′-*O* adduct profile in region III/IV/V (Fig. 1), suggesting an alternative conformation. This notion was supported by the folding algorithm when constrained by our SHAPE data.

NMIA reactivity profiles were superimposed on the secondary structure model of RRE61 RNA (Fig. S3) and the two G:A mutations highlighted as open circles (Fig. 3). Comparing models of the native (Fig. 2) and RRE61 RNAs (Fig. 3) indicated that while regions I and IIA/IIB/IIC are identical, region III/IV/V was significantly altered. In particular, the extended stem-loop III/IV (Fig. 2) was resolved into two stem loops (defined here as III and extended IV), whereas stem V decreased by 4 bp (Fig. 3). High to moderate NMIA reactivity was again observed in mainly single-stranded regions, outlining loops, bulges, and junctions of RRE61. One striking feature was a lack of reactivity at the 195–196, 214–215 bulge in extended stem IV. However, precedents for noncanonical, structurally-important C-A and G-A base pairs have been demonstrated in catalytic RNA (21, 22).

Effect of Individual RRE Mutations. Because two G ->A mutations allow RRE61 RNA to adopt a new configuration in region III/IV/V, we evaluated the contribution of each to RRE structure and RevM10 resistance. The mutations were individually introduced into a proviral clone to produce viruses that were grown in the presence of RevM10. Virus containing the G:A245 mutation replicated well, indicating that it alone was sufficient to convey most of the RevM10-resistance, although these viruses replicated less well than the double RRE61 mutant. The G:A164 mutant and WT virus were RevM10-sensitive, although in this experiment some breakthrough growth was seen in both cultures at 21 days (Fig. 4). Thus, G:A 164 may contribute somewhat to resistance in combination with G:A254 but not by itself. In a control experiment, the replication capability of each HIV-1 variant in the absence of RevM10 was similar (Fig. S4).

We next probed the contribution of each mutation to RRE structure. RNAs were folded and resolved by nondenaturing polyacrylamide gel electrophoresis. Mutant G:A164 migrated analogous to the native RRE, and mutant G:A245 to RevM10-resistant RRE61 (Fig. S5). SHAPE experiments and comparative step plots were performed to analyze the two mutants. When the profiles of the RRE61 and the G:A245 RNAs were superimposed, no significant changes were observed (Fig. 5*A*). As expected, the folding algorithm constrained by SHAPE had indicated a secondary structure in which stem IV was extended by 4 bp, whereas stem V was decreased by the same amount (Fig. 5*C*). Thus, *in vitro* replication kinetics, native gel analysis and

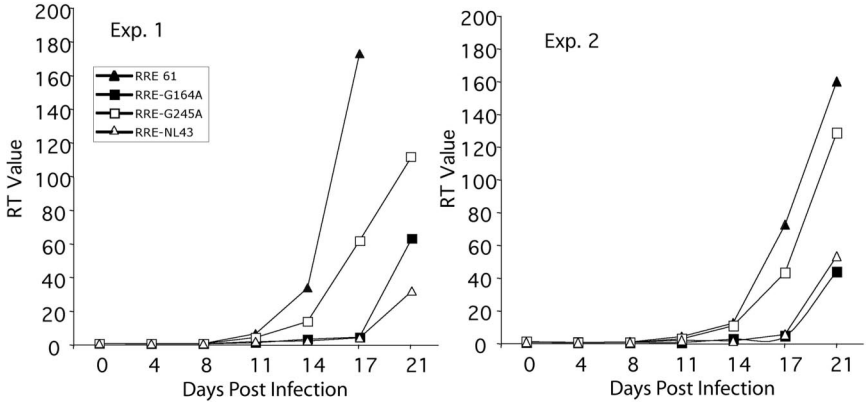

Fig. 4. Replication of HIV with altered RREs in CEM/14M10B cells. Supernatants from 293 T cells transfected with NL4–3 proviral clones containing WT or variant RREs were used to infect CEM/14M10B cells. Replication was determined by measuring supernatant RT activity. Input virus was standardized using the RT activity of the supernatant. Data are from two separate experiments.

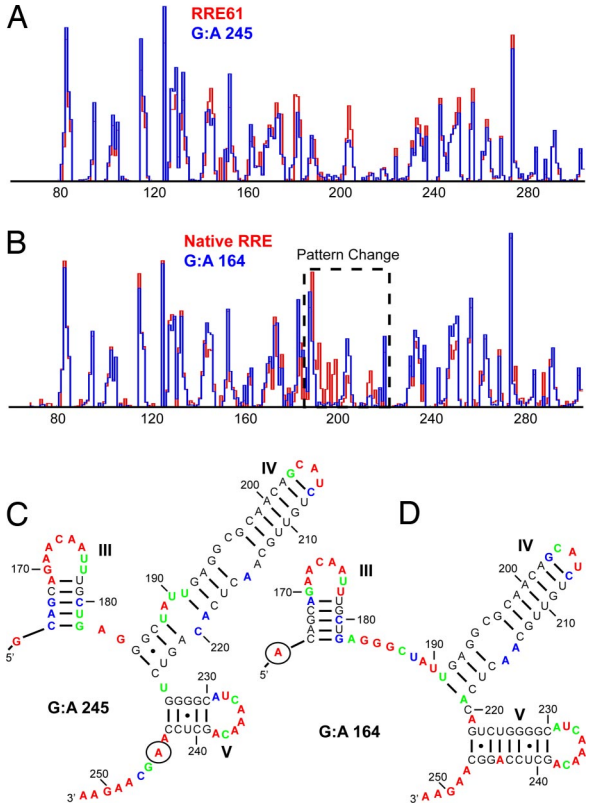

Fig. 5. SHAPE analysis of RREs with individual G:A245 and G:A164 mutations. (*A* and B) Quantitative comparison step plots of RRE61 vs. G:A245 and RRE vs. G:A164, respectively. (*C* and *D*) Secondary structures of region III/IV/V of the G:A245 and G:A164 mutants, respectively. NMIA reactivity is color-coded as in Fig. 2 and 3.

chemical footprinting clearly indicate that the G:A245 mutation alone suffices to mimic the RRE61 structure.

When the NMIA reactivity profiles of the native RRE and mutant G:A164 were superimposed, significant differences were observed, suggesting this RNA adopted another conformation (Fig. 5*B*). The folding algorithm constrained by SHAPE predicted a two stem-loop motif for extended loop IV (Fig. 5*D*) that was significantly shorter than the equivalent motif of RRE61 and mutant G:A245. At the same time, stem-loop V resembled that of the WT RRE. Taken together, these observations demonstrate that mutant G:A164 adopts a hybrid structure combining features of the WT and RevM10-resistant RREs.

Monitoring Rev Binding by Mass Spectrometry and Chemical Footprinting. We next used FT-ICR mass spectrometry to examine if the stoichiometry of Rev binding to WT and RRE61 RNAs was affected. The RNAs initially appear in two ionization states corresponding to a mass of ≈89 kDa (Fig. 6 *A* and *B*). Titrating Rev onto the RRE resulted in additional peaks corresponding to masses of ≈102, 115, and 128 kDa. The mass increment of each peak was ≈13 kDa, i.e., that of a Rev monomer. Mass spectrometry thus provided a convenient means of directly assessing Rev stoichiometry. Surprisingly, no significant difference in Rev binding to the WT and mutant RNAs was observed.

The effect of Rev binding to native and RRE61 RNA was also monitored by SHAPE (Fig. 6 *C* and *D*). Similar changes in NMIA reactivity were observed in both stem I and region IIA/IIB/IIC. In stem I, many nucleotides in the bulge containing nucleotides 83–86, 263–265 became constrained. In region IIA/IIB/IIC, previously flexible nucleotides at positions 103–106, 126, 129, and 131 become constrained, corresponding with previous NMR assignments (23) defining the primary Rev binding site. Moreover, nucleotides 133 and 134 also become constrained. Strikingly, many of the constrained positions along with nucleotides 133 and 134 lie on the same face of the RNA (Fig. S6) suggesting the N terminus of the arginine-rich region in the NMR structure affords additional protection. Because we are using full-length Rev and not the arginine-rich peptide examined by NMR, we infer that another region of Rev may lie next to this RNA face. Rev also induces similar global effect on both RNAs in region IIA/IIB/IIC. Positions 102, and 154–157 are more flexible, highlighting that protein binding induces stem IIA to melt by 2 bp.

The similarity between RRE and RRE61 RNA in their primary Rev binding site and in stem I suggest binding is not influenced by the alternative structure assumed by the latter. However, NMIA reactivity at several positions in region III/IV/V of the WT RRE is modified when this region is resolved into in the individual stem-loops of RRE61 (Fig. 6 *C* and *D*). This was particularly evident for nucleotides 238 and 236, which become more constrained. We also observed that nucleotides 95 and 96 are more flexible after Rev binding.

Interaction of RevM10 with RRE and RRE61. Since few differences between Rev binding to RRE and RRE61 were noted, we considered the possibility that RevM10 resistance reflected the manner in which the WT and RRE61 RNAs bound the mutant protein. SHAPE experiments were repeated using purified RevM10. However, equivalent regions of enhanced or reduced NMIA susceptibility were observed on both RRE and RRE61, regardless of the protein source (data not shown).

Discussion

Structural Basis of RevM10 Resistance. The significance of adopting different conformations in region III/IV/V of the HIV-1 RRE on virus replication is not immediately clear. However, two silent mutations underlying RevM10 resistance may offer some insight. In the study in ref. 17, of nine clones derived from resistant virus arising after passage in cells expressing RevM10, all contained the G:A164 mutation, whereas three had the additional G:A245 mutation and 3 had changes that led to changes in the envelope protein sequence. The three mutations that changed the envelope protein sequence failed to grow when built back into virus and thus were not studied further (ref. 17 and T.E.H., D.R. and M.-L.H. unpublished data). Although a small sampling, this distribution makes a strong case that the G:A164 mutation arose first. However, when this mutation was introduced into pNL4–3 and virus was grown in cells expressing RevM10, its replication kinetics (Fig. 4) was not very different from the WT virus.

Analysis of the prototype sequences in the HIV sequence database reveals that G at position 164 of the RRE is present only in a few of the clade B isolates (≈15%). The predominant residue at that position is usually an A. Thus, the NL4–3 RRE appears to change to the more common sequence, before selecting the G:A245 mutation.

Our structural data indicates that the G:A164 mutation enforces a two stem loop motif in region III/IV of the RNA (Fig. 5 *B* and *D*). Initial exposure to RevM10 virus apparently selects for a mutation enforcing a two stem-loop motif (Fig. S7). However, the motif induced by the G:A164 mutation is not the same structure observed in RRE61, but a hybrid of the native RRE and RRE61 (Fig. S7). One possibility is that by adopting a G:A164 mutation, sufficient low-level virus replication to acquire the second, G:A245, mutation is permitted, leading to RevM10 resistance by adopting the final RRE61 structure. Strikingly, by employing only two silent mutations, NL4–3 can alter RRE structure without expending much energy in the process. Moreover, retention of the G:A164 mutation does not

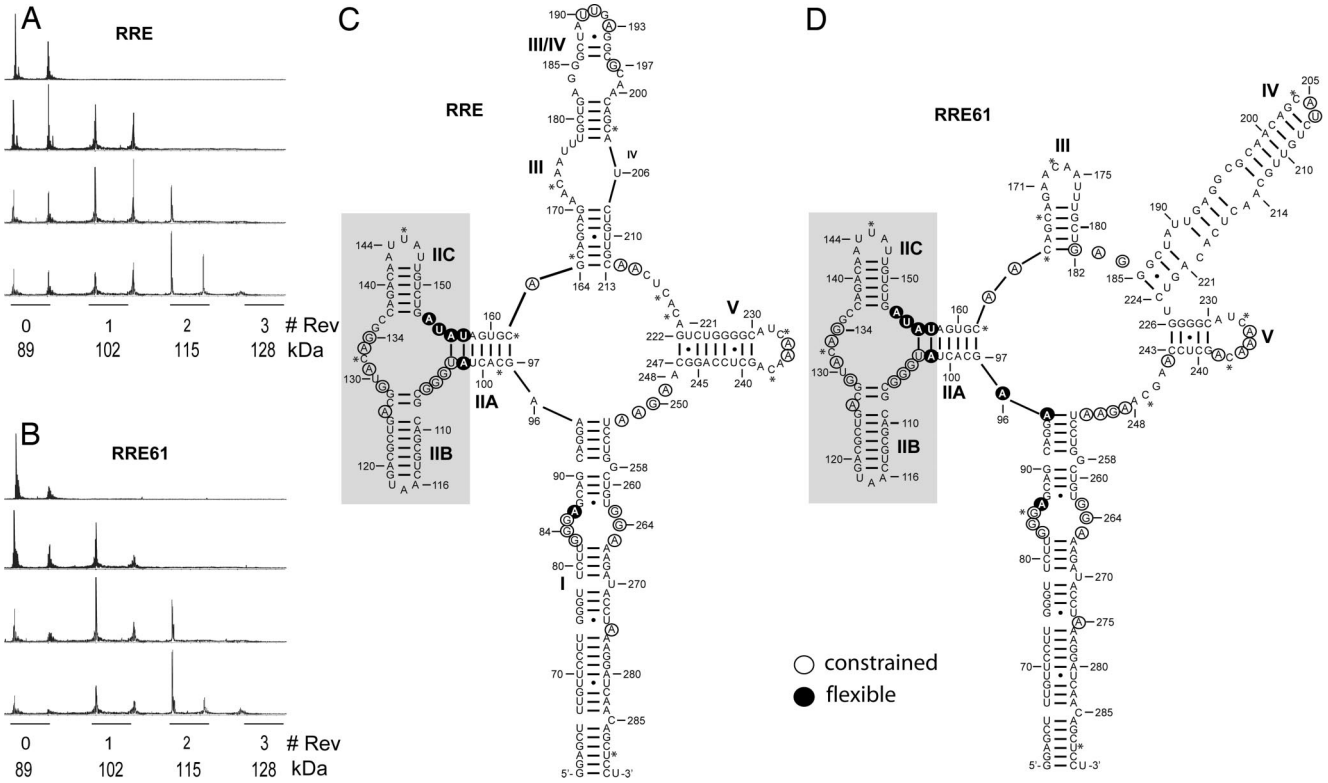

Fig. 6. Effects of Rev binding on the native and RRE61 RNAs. (*A* and *B*) ESI-MS analysis of RRE and RRE61, respectively. (*C* and *D*) NMIA footprinting. Nucleotides that are constrained or flexible on Rev binding are indicated by open and closed circles, respectively. The shaded box is the primary Rev binding site.

appear critical, because SHAPE analysis suggests that the G:A245 mutation alone induces the same structure (Fig. 5*C*) and confers equivalent RevM10 resistance as RRE61 (Fig. 4). Our data also imply that isolates of HIV-1 that already have the A mutation at position 164, may be able to more readily develop resistance.

Rev Binds the RRE in Monomeric Increments. Current literature suggests that HIV-1 Rev interacts with nucleotides 103–106 and 123–131 (23) of RRE region IIA/IIB/IIC, then multimerizes (10), using domains flanking the NLS, and ultimately binds secondary targets in other regions, in particular stem I. We therefore asked whether Rev binds the RRE as a monomer or in a multimeric state and whether structural changes in RRE61 influenced Rev binding. RRE and RRE61, with masses of ≈89 kDa, are among the largest RNAs to be analyzed by mass spectrometry. When we add Rev at a 1:1 protein:RNA ratio, a new peak of mass ≈102 kDa indicates that Rev initially associates with the RRE as a monomer. Increasing Rev concentration led to new peaks whose mass increments again correspond to momomeric Rev. However, we cannot discern if additional molecules multimerize with the primary Rev or bind elsewhere on the RRE. Regardless, our data suggest that Rev multimerization is dependent on the RRE because mass spectrometry indicates the free protein exists in a monomeric state under the conditions we have used (data not shown).

Despite the altered RRE61 structure, Rev occupancy of branched stem-loop IIA/IIB/IIC was unaffected. At the same time, significant structural changes between RRE and RRE61, in particular rearrangement of region III/IV into individual stem-loops III and IV, prevent a direct comparison of potential secondary binding sites. However, acylation sensitivity at the apex of stem-loop III/IV of the WT RRE suggests another site may be occupied at elevated Rev concentrations. Saturation of the region surrounding the primary Rev binding site (branched stem-loop IIA/IIB/IIC) could globally affect RRE structure, allowing this and stem-loop III/IV to be "bridged" by an additional Rev molecule as a means of presenting a new binding surface to accessory factors involved in RNA export. If the structure adopted by RRE61 sufficed to bind accessory proteins in lower levels of functional Rev, the inhibitory effect of RevM10 would be negated. This hypothesis also implies that RevM10 interrupts bridging, rather than the primary Rev binding event.

Although the use of subgenomic heterologous reporter constructs suggest stem-loop II is the only region required for Rev function (24, 25), other studies, using less artificial constructs, highlight the importance of sequences throughout the RRE (26–31). For example, mutations that disrupt the stem of stem-loop V create a nonfunctional RRE in both HIV-1 (26) and HIV-2 (31). Another study, using oligonucleotides complementary to the stem of stem-loop V, showed that such oligonucleotides were 9-fold more active in blocking Rev-RRE function *in vivo* compared with oligonucleotides directed to the primary Rev binding site, i.e., stem loop II (32). In addition, Rev also has cytoplasmic affects on HIV RNA utilization (33, 34), supporting the view that Rev and RRE function is more complicated than the simple model that it merely serves as an adapter to bring CRM1 to the RNA cargo. Many of these studies have used HIV virus or constructs that make intact unchanged HIV proteins from genuine viral mRNAs. Finally, although our observations indicate the Rev/RRE system merits further examination, the notion that silent nucleotide changes have such a dramatic effects on structure and function suggests the RRE could adapt to alter the level of virus expression as suggested (35).

Experimental Procedures

Retroviral RNAs. RNAs were prepared by *in vitro* transcription, using the MEGAshortscript T7 Kit (Ambion). RNAs were purified by denaturing gel

electrophoresis (5% polyacrylamide, 7 M urea), eluted, precipitated, resuspended in TE buffer [10 mM Tris (pH 7.4), 0.1 mM EDTA], and stored at −20°C.

Renaturation, Rev Binding, and NMIA Treatment of RNAs. For normalization, RRE RNAs had a 3′ nonviral RNA cassette containing an efficient primer binding site. RNAs (20 pmol) were heated at 90°C for 3 min in 20 μl of 10 mM Tris·HCl (pH 8.0), 100 mM KCl, and 0.1 mM EDTA, cooled to 4°C, mixed with 29 μl of 5× Rev binding buffer [200 mM Tris·HCl (pH 8.0), 0.65 M KCl, 22.5 mM $MgCl_2$, 5 mM DTT, 2.5 mM EDTA, 500 μg/ml BSA, 25% glycerol] and 13.1 μl of Rev storage buffer [50 mM Tris·HCl (pH 8.0), 0.3 M NaCl, 0.1 mM EDTA] alone or in the presence of Rev (0.5 mg/ml, 500 pmol final), brought up to 145 μl with ddH_20, and incubated at 37°C for 10 min. Samples were treated with 7.3 μl of 180 mM NMIA (in anhydrous DMSO) or DMSO alone at 37°C for 50 min, precipitated and extracted with 200 μl of phenol:chloroform:isoamyl alcohol (25:24:1). The aqueous layer was retained and treated again with 200 μl of chloroform (Sigma), and the RNA was precipitated and resuspended in 10 μl of TE buffer.

Primer Extension. Reactions were performed as described in ref. 18 except that 0.5 μl (100 units) of SuperScript III RT (Invitrogen) was added. 5′-end-labeled DNA primers complementary to the 3′ end of the RNA cassette (5′-GAACCGGACCGAAGCCCG-3′) and a portion of region III/IV starting at nucleotide 203 (5′-CTGTTGCGCCTCAATAGCCCT-3′) were used to analyze the entire RRE RNA. A stochastic drop-off was observed and reactivities were adjusted as described in ref. 37.

Replication of HIV with Altered RREs in CEM/14M10B Cells. Supernatants from 293 T cells transfected with NL4–3 proviral clones containing WT or variant RREs were used to infect 5×10^6 CEM/14M10B cells in a 5-ml culture. Input virus was normalized using RT activity of the supernatant. Cultures were sampled for p24 activity released into the medium every 3–4 days, at which time, 3 ml was removed and replaced with fresh medium. CEM/14M10B cells are a clonal isolate of CEM cells containing a modified LXSN retroviral vector expressing RevM10.

Rev Binding and Isomerization Experiments. All experiments were performed using 10–15 μM solutions of each RNA by dilution of stock solutions into 180 mM ammonium acetate (pH 7.0). Before use, samples were heated to 95°C for 5 min. and slowly cooled to allow proper folding. Binding experiments were initiated by adding Rev at room temperature to a final RNA:protein ratio of 1:1, 1:3, and 1:5.

Mass Spectrometry. Analyses were performed on a Bruker Daltonics Apex III FTICR mass spectrometer equipped with a 7T actively-shielded superconducting magnet and a nano-ESI source. Desolvation temperature, skimmer voltage, and other source parameters were optimized for observing intact, noncovalent protein-RNA complexes (36). Analyte solutions were mixed with iso-propanol before analysis (final concentration 10% vol/vol) to assist desolvation. Five-μl samples were loaded into the nano-electrospray needle, and a spray voltage of <1 kV was applied to the solution through a stainless steel wire. Spectra were acquired in negative ionization mode and processed using XMASS 7.0.2 (Bruker Daltonics). Scans were completed in broadband mode that allowed for a typical 150,000 resolving power at *m/z* 2,000.

ACKNOWLEDGMENTS. This work is supported by the intramural research program of the National Institutes of Health (S.F.J.L.G.); National Institutes of Health Grants AI054335 (to D.R.), AI068501 (to M.-L.H.), and GM643208 (to D.F.); and the Myles H. Thaler and Charles Ross, Jr. Eminent Scholar Professorships at the University of Virginia (to D.R. and M.-L.H).

1. Fakuda M, *et al.* (1997) CRM1 is responsible for intracellular transport mediated by the nuclear export signal. *Nature* 390:308–311.
2. Fornerod M, Ohno M, Yoshida M, Mattaj M (1997) CRM1 is an export receptor for leucine-rich nuclear export signals. *Cell* 90:1051–1060.
3. Arnold M, Nath A, Hauber J, Kehlenbach RH (2006) Multiple importins function as nuclear transport receptors for the Rev protein of human immunodeficiency virus type 1. *J Biol Chem* 281:20883–20890.
4. Ruhl M, *et al.* (1993) Eukaryotic initiation factor 5A is a cellular target of the human immunodeficiency virus type 1 Rev activation domain mediating trans-activation. *J Cell Biol* 123:1309–1320.
5. Zapp ML, Green MR (1989) Sequence-specific RNA binding by the HIV-1 Rev protein. *Nature* 342:714–716.
6. Perkins A, Cocrane AW, Ruben SM, Rosen CA (1989) Structural and functional characterization of the human immunodeficiency virus rev protein. *J Acquired Immune Deficiency Syndrome* 2:256–263.
7. Kjems J, Calnan BJ, Frankel AD, Sharp PA (1992) Specific binding of a basic peptide from HIV-1 Rev. *EMBO J* 11:1119–1129.
8. Tan R, Chen L, Buettner JA, Hudson D, Frankel AD (1993) RNA recognition by an isolate α helix. *Cell* 73:1031–1040.
9. Zapp ML, Hope TJ, Parslow TG, Green MR (1991) Oligomerization and RNA binding domains of the type 1 human immunodeficiency virus Rev protein: A dual function for an arginine-rich binding motif. *Proc Natl Acad Sci USA* 88:7734–7738.
10. Jain C, Belasco JG (2001) Structural model for the cooperative assembly of HIV-1 Rev multimers on the RRE as deduced from analysis of assembly-defective mutants. *Mol Cell* 7:603–614.
11. Hope TJ, Bond BL, McDonald D, Klein NP, Parslow TG (1991) Effector domains of human immunodeficiency virus type 1 Rev and human T-cell leukemia virus type I Rex are functionally interchangeable and share an essential peptide motif. *J Virol* 65:6001–6007.
12. Malim MH, Bohnlein S, Hauber J, Cullen BR (1989) Functional dissection of the HIV-1 Rev trans-activator-derivation of a trans-dominant repressor of Rev function. *Cell* 58:205–214.
13. Bevec D, Dobrovnik M, Hauber J, Böhnlein E (1992) Inhibition of human immunodeficiency virus type 1 replication in human T cells by retroviral-mediated gene transfer of a dominant-negative Rev trans-activator. *Proc Natl Acad Sci USA* 89:9870–9874.
14. Bahner I, *et al.* (2007) Lentiviral vector transduction of a dominant-negative. Rev gene into human $CD34^+$ hematopoietic progenitor cells potently inhibits human immunodeficiency virus-1 replication. *Mol Ther* 15:76–85.
15. Cordelier P, Van Bockstaele E, Calarota SA, Strayer DS (2003) Inhibiting AIDS in the central nervous system: Gene delivery to protect neurons from HIV-1. *Mol Ther* 7:801–810.
16. Strayer, *et al.* (2002) Combination genetic therapy to inhibit HIV-1. *Mol Ther* 5:33–41.
17. Hamm TE, Rekosh D, Hammarskjöld ML (1999) Selection and characterization of human immunodeficiency virus type 1 mutants that are resistant to inhibition by the transdominant negative RevM10 protein. *J Virol* 73:5741–5747.
18. Wilkinson KA, Merino EJ, Weeks KM (2006) Selective 2′-hydroxyl acylation analyzed by primer extension (SHAPE): Quantitative RNA structure analysis at single nucleotide resolution. *Nat Protoc* 1:1610–1616.
19. Charpentier B, Stutz F, Rosbash M (1997) A dynamic in vivo view of the HIV-1 Rev-RRE interaction. *J Mol Biol* 266:950–962.
20. Kjems J, Brown M, Chang DD, Sharp PA (1991) Structural analysis of the interaction between the human immunodeficiency virus Rev protein and the Rev response element. *Proc Natl Acad Sci USA* 88:683–687.
21. Cate JH, *et al.* J.A (1996) Crystal structure of a group I ribozyme domain: Principles of RNA packing. *Science* 273:1678–1685.
22. Lescrinier EM, *et al.* (2003) Structure of the pyrimidine-rich internal loop in the poliovirus 3′-UTR: The importance of maintaining pseudo-2-fold symmetry in RNA helices containing two adjacent non-canonical base-pairs. *J Mol Biol* 331:759–769.
23. Battiste JL, *et al.* (1996) A helix-RNA major goove recognition in an HIV-1 Rev peptide-RRE RNA complex. *Science* 273:1547–1551.
24. Huang XJ, *et al.* (1991) Minimal Rev-response element for type 1 human immunodeficiency virus. *J Virol* 65:2131–2134.
25. McDonald D, Hope TJ, Parslow TG (1992) Posttranscriptional regulation by the human immunodeficiency virus type 1 Rev and human T-cell leukemia virus type I Rex proteins through a heterologous RNA binding site. *J Virol* 66:7232–7238.
26. Dayton ET, *et al.* (1992) Extensive sequence-specific information throughout the CAR/RRE, the target sequence of the human immunodeficiency virus type 1 Rev protein. *J Virol* 66:1139–1151.
27. Dayton ET, Powell DM, Dayton AI (1989) Functional analysis of CAR, the target sequence for the Rev protein of HIV-1. *Science* 246:1625–1629.
28. Holland SM, Ahmad N, Maitra RK, Wingfield P, Venkatesan S (1990) Human immunodeficiency virus Rev protein recognizes a target sequence in the Rev-responsive element RNA within the context of RNA secondary structure. *J Virol* 64:5966–5975.
29. Malim MH, *et al.* (1990) HIV-1 Structural gene expression requires binding of the Rev trans-activator to its RNA target sequence. *Cell* 60:675–683.
30. Olsen HS, Nelbock P, Cochrane AW, and Rosen CA (1990) Secondary structure is the main determinant for interaction of HIV Rev protein with RNA. *Science* 247.
31. Dillon PJ, Nelbock P, Perkins A, Rosen CA (1990) Function of the human immunodeficiency virus types 1 and 2 Rev proteins is dependent on their ability to interact with a structured region present in env gene mRNA. *J Virol* 64:4428–4437.
32. Fenster SD, Wagner RW, Froehler BC, Chin DJ (1994) Inhibition of human immunodeficiency virus type-1 env expression by C-5 propyne oligonucleotides specific for Rev-response element stem-loop V. *Biochemistry* 33:8391–8398.
33. D'Agostino DM, Felber BK, Harrison JE, Pavlakis GN (1992) The Rev protein of human immunodeficiency virus type 1 promotes polysomal association and translation of gag/pol and vpu/env mRNAs. *Mol Cell Biol* 12:1375–1386.
34. Swanson CM, Puffer BA, Ahmad KM, Doms RW, Malim MH (2004) Retroviral mRNA nuclear export elements regulate protein function and virion assembly. *EMBO J* 23:2632–2640.
35. Phuphuakrat A, Auewarakul P (2005) Functional variability of Rev response element in HIV-1 primary isolates. *Virus Genes* 30:23–29.
36. Turner KB, Hagan NA, Fabris D (2007) Understanding the isomerization of the HIV-1 dimerization initiation domain by the nucleocapsid protein. *J Mol Biol* 369:812–818.
37. Badorrek CS, Weeks KM (2006) Architecture of a gamma retroviral genomic RNA dimer. *Biochemistry* 45:12664–12672.